A Simple Model Predictive Power Control Strategy for Single-Phase PWM Converters With Modulation Function Optimization

Wensheng Song, *Member, IEEE*, Zhixian Deng, Shunliang Wang, and Xiaoyun Feng

***Abstract*—This paper proposes a simple model predictive direct power control (MP-DPC) of single-phase pulsewidth-modulated rectifiers with constant switching frequency using modulation function optimization. The instantaneous active and reactive power theory for single-phase converters is discussed, on the basis of a second-order generalized integrator. The modulation function is resolved from the cost function of the MP-DPC scheme. The relationship between the instantaneous powers and ac-side inductance mismatch is discussed. The inductance mismatch has an effect on the reactive power, but not effect on active power. The quantitative expression of reactive power caused by inductance mismatch is shown and verified in the experimental test. An inductance parameter online estimation scheme is proposed to eliminate its effect on reactive power. Compared with the conventional proportional-integral-based instantaneous current control scheme and finite-control-set MP-DPC scheme, the proposed MP-DPC can provide these advantageous features: lower current harmonics and total harmonic distortion components, faster dynamic response, fewer adjusted parameters, and zero steady-state error. In addition, the proposed MP-DPC is free of the weighting factor selection in cost function. The effectiveness of the proposed MP-DPC scheme is verified by experimental results.**

***Index Terms*—Single-phase rectifier, model predictive power control, modulation function optimization, parameter sensitivity, pulsewidth-modulation (PWM).**

I. Introduction

POWER pollution, due to the wide application of diode or thyristor converters, has been a serious power-quality problem. Thus, in recent years, a single-phase voltage source converter based on pulsewidth modulation (PWM) schemes, has been widely utilized in many grid-interfaced systems, e.g., renewable energy source generation [1], power factor controllers [2], uninterruptible power supply [3], railway electrical traction transportation [4], [5]. Because it can obtain the better performance characteristics, such as high power factor, low current harmonics distortion, and bidirectional energy flow, as compared with diode or thyristor converters.

In order to achieve a sinusoidal line current with a near unity power factor and obtain a constant dc-link voltage, various control strategies have been proposed for single-phase PWM converters, which can be categorized into two major classes, namely, current-based control [6]–[13] and direct power control (DPC) [14]–[16]. The current-based control scheme is widely reported and utilized in single-phase PWM converters application, which commonly includes indirect current control [6], hysteresis control [7], proportional-integral (PI)-based [8] or proportional-resonant (PR)-based [9], [10] instantaneous current control (ICC), voltage-oriented control (VOC) [11], and predictive control [12]. Whatever, the essential goal of the current-based control scheme is to solve a current tracking problem, i.e., the grid-side current is forced to track the current reference, which is defined as a signal proportional to the fundamental component of the grid voltage by phase-lock loop (PLL) technology. Currently, PI-based ICC schemes are widely adopted for single-phase PWM converters in railway traction application [5], [13]. One of PI-based ICC scheme drawbacks is that the ac-side current exits steady-state error due to the adopted PI controller for grid-side current with 50/60 Hz. Another drawback is the complicated choice and tuning of current's PI parameters. The VOC scheme in [11] and PR-based ICC in [9] and [10] are proposed to eliminate the steady-state error, respectively. However, compared with the traditional PI-based ICC, VOC scheme requires more PI controllers, and the PR-based ICC scheme is very sensitive and dependent on the choice of resonance parameters.

The DPC approach is a well-known efficient control strategy for power converters based on the instantaneous power theory reported in [17], which originates from the well-known direct torque control (DTC) used in adjustable speed drives system. The DPC algorithm directly uses the instantaneous active and reactive power terms as control variables to replace the current variables that are commonly used in an VOC system [11], which is similar to application of stator flux and torque terms as control variables in DTC. In recent years, DPC approaches are widely reported and applied in three-phase converters [18]–[37]. Being similar to direct current control, the DPC scheme commonly includes hysteresis lookup-table control [18]–[20], fuzzy-logic lookup-table control [21], PI-based linear power control [26], [27], sliding model nonlinear control [28], deadbeat predictive control [29]–[31], and model predictive control [32]–[41].

Manuscript received May 6, 2015; revised July 26, 2015; accepted September 15, 2015. Date of publication September 23, 2015; date of current version January 28, 2016. This work was supported in part by the National Natural Science Foundation of China under Projects 51207131, 51277153, and 51577160 and in part by the National High Speed Railway Joint Key Foundation of China under Project U1134205. Recommended for publication by Associate Editor Ray-Lee Lin.

W. Song, Z. Deng, and S. Wang are with the School of Electrical Engineering, Southwest Jiaotong University, Chengdu 610031, China (e-mail: songwsh@swjtu.edu.cn; 449004043@qq.com; shunliangwang@my.swjtu.edu.cn).

X.Feng is with State Key Laboratory of Traction Power, Southwest Jiaotong University, Chengdu 610031, China (e-mail: fengxy@swjtu.edu.cn).

Color versions of one or more of the figures in this paper are available online at http://ieeexplore.ieee.org.

Digital Object Identifier 10.1109/TPEL.2015.2481323

Recently, with the development of digital signal processing technology, predictive control schemes are widely applied in power converters. Deadbeat predictive control and model predictive control are two well-known approaches. The former uses a predictive model of the system to calculate the required reference voltage during a control period in order to reach the desired reference value for the variables such as: currents, active and reactive powers [29]–[31]. And the latter uses the system model to predict the behavior of the variables over a control period, and a cost function is defined as a criterion, and the cost function minimization is adopted to select the optimal future actions [33], [42]–[44]. MPC has several advantages, such as the fast dynamic response, the easy inclusion of nonlinearities and constraints.

Although the model predictive direct power control (MP-DPC) has been extensively investigated for three-phase power converters, a few approaches have been developed for single-phase converters [15]. The classical MP-DPC scheme is discussed in [15], which can obtain a fast dynamic response. But the main drawback is to obtain variable switching frequency. In three-phase converters, MP-DPC with space vector PWM (SVPWM) [26], [29], or discrete SVPWM [44] schemes are proposed to solve this problem. As is well known, the parameter sensitiveness problem is the main drawback of model predictive control. Although literatures [39], [42], [43] have reported the analysis and compensation solution of inductor parameter mismatch in these MP-DPC schemes. But the quantitative relationship between instantaneous powers and ac-side inductance mismatch has not been reported until now. Therefore, from the modulation function point of view, this paper presents a simple MP-DPC using modulation function optimization with carrier-based PWM (CBPWM), for single-phase PWM rectifiers, to gain constant switching frequency. The parameter sensitivity of ac-side inductance mismatch is analyzed in detail. The quantitative expression of reactive power caused by inductance mismatch is deduced. In addition, an inductance online estimation method is proposed to eliminate the effect on reactive power. A performance comparison of the proposed MP-DPC, PI-based ICC, and finite-control-set (FCS) MP-DPC [43] schemes is adopted in the experimental test.

This paper is organized in the following manner. The system configuration of the adopted single-phase PWM rectifier is discussed in Section II. The single-phase instantaneous powers theory is provided in Section III. The model predictive power control algorithm and inductance sensitiveness analysis and compensation are presented in Section IV. The experimental results are presented and discussed in Section V, followed by a conclusion in Section VI.

II. System Configuration of Single-Phase PWM Rectifiers

A single phase two-level PWM converter is depicted in Fig. 1, where L and R are symbols for the equivalent inductance and resistance of ac-side inductor, respectively; and it is assumed that a pure resistive load R_L is connected at the dc-link capacitor C_d. Four active switches S_1, S_2, S_3, and S_4 are used in the adopted converter to generate two voltage levels on the converter's leg-a and leg-b, respectively.

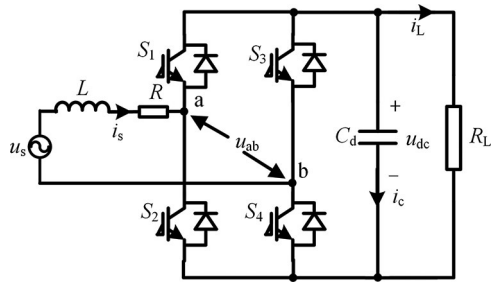

Fig. 1. Topology of a single-phase PWM converter.

Applying the Kirchhoff voltage law to analyze the voltage across inductor L yields

$$L\frac{di_s}{dt} = u_s - u_{ab} - i_s R \tag{1}$$

where u_s, i_s, and u_{ab} represent the main voltage, the line current, and the input voltage of the adopted converter, respectively. u_s and i_s are defined as

$$u_s = U_{sm}\cos(\omega t) \tag{2}$$

$$i_s = I_{sm}\cos(\omega t - \varphi) + \sum_{k=3(\text{odd})}^{\infty} I_{smk}\cos(k\omega t - \varphi_k) \tag{3}$$

where U_{sm} and I_{sm} are the peak values of the fundamental components in the main voltage and the line current, respectively; ω is the angular frequency of the main voltage; and φ is the displacement power factor angle. The second component in the right side of (3) represents the harmonic components in the line current.

III Single-Phase Active and Reactive Powers Theory in Virtual Two-Axis Reference Frame

On the basis of (2) and (3), and neglecting the harmonic currents' effect, the active and reactive power expressions for the single-phase PWM converter can be written as

$$\begin{cases} P = \dfrac{U_{sm} I_{sm}\cos\varphi}{2} \\ Q = \dfrac{U_{sm} I_{sm}\sin\varphi}{2}. \end{cases} \tag{4}$$

As is well known, it is a common practice to transform three-phase power converter systems into the two-axis stationary (α–β) or rotary (d–q) reference frames. These transformations bring significant simplicity and ease of analysis, especially when determining the instantaneous active and reactive powers in three-phase systems. Hence, a virtual two-phase system should be constructed for single-phase converters application. Recently, the generation methods of a fictitious orthogonal phase component from a single-phase quantity are widely reported, such as 90° phase shift [45], Hilbert transformation [46], all-pass filter [47], and second-order generalized integrator (SOGI) [16], [48]. The SOGI is an advanced and popular orthogonal signal generation technique. The characteristic transfer function of SOGI in

s-domain [16] can be described as

$$\begin{cases} x_\alpha(s) = \dfrac{k\omega s}{s^2 + k\omega s + \omega^2} x(s) \\ x_\beta(s) = \dfrac{k\omega^2}{s^2 + k\omega s + \omega^2} x(s) \end{cases} \tag{5}$$

where k is the damping factor, the outstanding performance of SOGI depends on the selection of damping factor k. The SOGI can filter the harmonics being away from the central frequency ω.

From (5), it is clear that the SOGI can effectively extract the fundamental components from the original signals with harmonics. Applying (5) to the main voltage u_s and the line current i_s, respectively, the fundamental component expressions of u_s and i_s in virtual two-axis (α–β) reference frame are shown as

$$\begin{cases} u_{s\alpha} = u_s = U_{sm}\cos(\omega t) \\ u_{s\beta} = U_{sm}\sin(\omega t) \end{cases} \tag{6}$$

$$\begin{cases} i_{s\alpha} = i_s = I_{sm}\cos(\omega t - \varphi) \\ i_{s\beta} = I_{sm}\sin(\omega t - \varphi). \end{cases} \tag{7}$$

Then, on the basis of the active and reactive powers in (4), the active and reactive powers in α–β reference frame can be expressed as

$$\begin{cases} P = \dfrac{U_{sm} I_{sm}\cos\varphi}{2} = \dfrac{u_{s\alpha} i_{s\alpha} + u_{s\beta} i_{s\beta}}{2} \\ Q = \dfrac{U_{sm} I_{sm}\sin\varphi}{2} = \dfrac{u_{s\beta} i_{s\alpha} - u_{s\alpha} i_{s\beta}}{2}. \end{cases} \tag{8}$$

The differentiations of active power P and reactive power Q with respect to time t can be obtained from (8) as

$$\begin{cases} \dfrac{dP}{dt} = \dfrac{1}{2}\left(u_{s\alpha}\dfrac{di_{s\alpha}}{dt} + i_{s\alpha}\dfrac{du_{s\alpha}}{dt} + u_{s\beta}\dfrac{di_{s\beta}}{dt} + i_{s\beta}\dfrac{du_{s\beta}}{dt}\right) \\ \dfrac{dQ}{dt} = \dfrac{1}{2}\left(u_{s\beta}\dfrac{di_{s\alpha}}{dt} + i_{s\alpha}\dfrac{du_{s\beta}}{dt} - u_{s\alpha}\dfrac{di_{s\beta}}{dt} - i_{s\beta}\dfrac{du_{s\alpha}}{dt}\right). \end{cases} \tag{9}$$

The differentiations of currents $i_{s\alpha}$ and $i_{s\beta}$ with respect to time t can be also obtained from (1) and (7) as

$$\begin{cases} \dfrac{di_{s\alpha}}{dt} = \dfrac{1}{L}(u_{s\alpha} - u_{ab\alpha} - Ri_{s\alpha}) \\ \dfrac{di_{s\beta}}{dt} = \dfrac{1}{L}(u_{s\beta} - u_{ab\beta} - Ri_{s\beta}). \end{cases} \tag{10}$$

Substituting (6) and (10) into (9) yields

$$\begin{cases} \dfrac{dP}{dt} = \dfrac{1}{2L}\left[U_{sm}^2 - (u_{s\alpha}u_{ab\alpha} + u_{s\beta}u_{ab\beta}) - 2RP\right] - \omega Q \\ \dfrac{dQ}{dt} = -\dfrac{1}{2L}\left[(u_{s\beta}u_{ab\alpha} - u_{s\alpha}u_{ab\beta}) - 2RQ\right] + \omega P. \end{cases} \tag{11}$$

IV Proposed Model Predictive Power Control Scheme

A. Active and Reactive Power Prediction

The internal resistance R of an ac-side inductor is very small, and can be ignored. The active power $P(k+1)$ and reactive power $Q(k+1)$ at the $(k+1)$th sampling interval can be derived from (11) as

$$\begin{cases} P(k+1) = P(k) - \omega T_s Q(k) \\ \qquad + \dfrac{T_s}{2L}[U_{sm}^2 - u_{s\alpha}(k)u_{ab\alpha}(k) - u_{s\beta}(k)u_{ab\beta}(k)] \\ Q(k+1) = Q(k) + \omega T_s P(k) \\ \qquad - \dfrac{T_s}{2L}[u_{s\beta}(k)u_{ab\alpha}(k) - u_{s\alpha}(k)u_{ab\beta}(k)]. \end{cases} \tag{12}$$

B. Cost Function Optimization

The power control goal is that the instantaneous active power P and reactive powers Q are forced to track their references, P_{ref} and Q_{ref}. Therefore, following in model predictive theory, the cost functions must be relative to the active and reactive powers, which are usually defined as the following structures [39]–[43]:

$$J(k) = |P_{\mathrm{ref}}(k) - P(k+1)| + \lambda\,|Q_{\mathrm{ref}}(k) - Q(k+1)| \tag{13}$$

$$J(k) = |P_{\mathrm{ref}}(k) - P(k+1)|^2 + \lambda\,|Q_{\mathrm{ref}}(k) - Q(k+1)|^2 \tag{14}$$

where $P_{\mathrm{ref}}(k)$ and $Q_{\mathrm{ref}}(k)$ are the active and reactive reference powers at the kth sampling interval, respectively; λ represents the weighting factor of cost function. The optimization control object is to minimize the cost function $J(k)$ by selecting the appropriate switching modes of the adopted rectifier. The difference between (13) and (14) is that the latter produces an overproportional cost (in powers of two), producing a higher penalization of bigger errors compared with smaller ones. This can be used to control variables closer to the reference and reduce ripple amplitude. In essence, this error will produce a faster controller for the specific variable in the cost function. However, in the traditional finite-control-set (FCS) MP-DPC [43], it will also introduce higher switching frequencies. Therefore, the latter is widely adopted in MP-DPC with constant switching PWM module, and the former is widely used in FSC-MP-DPC. Of course, the former is ok in MP-DPC with constant switching PWM module. However, in this paper, in order to obtain a constant switching frequency and achieve the global optimization based on the PWM technology, we should calculate the differentiation of cost function with respect to the modulated signal. The differential process of cost function in (13) is very difficult, due to the expression type of the absolute value function. Four kinds of conditions should be considered to calculate the differentiation of (13) with respect to the modulated signal.

Thus, on the basis of the aforementioned two reasons, cost function in (14) is much appropriate in this paper. The optimization control object is to minimize the cost function $J(k)$ in (14) by selecting the appropriate control variables $u_{ab\alpha}(k)$ and $u_{ab\beta}(k)$, which yields

$$\begin{cases} \dfrac{\partial J(k)}{\partial u_{ab\alpha}(k)} = 0 \\ \dfrac{\partial J(k)}{\partial u_{ab\beta}(k)} = 0. \end{cases} \tag{15}$$

Substituting $P(k+1)$, $Q(k+1)$ of (12) and $J(k)$ of (14)into (15), the optimized control variables $u_{ab\alpha}(k)$ and $u_{ab\beta}(k)$ can be derived as

$$\begin{cases} u_{ab\alpha}(k) = u_{s\alpha}(k) - \dfrac{2Lu_{s\alpha}(k)}{T_s U_{sm}^2}\left[P_{\rm ref}(k) - P(k)\right] \\ \qquad + \dfrac{2Lu_{s\beta}}{T_s U_{sm}^2}\left[Q_{\rm ref}(k) - Q(k)\right] \\ \qquad + \dfrac{2L\omega}{U_{sm}^2}\left[P(k)u_{s\beta}(k) - Q(k)u_{s\alpha}(k)\right] \\ u_{ab\beta}(k) = u_{s\beta}(k) - \dfrac{2Lu_{s\beta}(k)}{T_s U_{sm}^2}\left[P_{\rm ref}(k) - P(k)\right] \\ \qquad + \dfrac{2Lu_{s\alpha}(k)}{T_s U_{sm}^2}\left[Q_{\rm ref}(k) - Q(k)\right] \\ \qquad - \dfrac{2L\omega}{U_{sm}^2}\left[Q(k)u_{s\beta}(k) + P(k)u_{s\alpha}(k)\right]. \end{cases} \tag{16}$$

And fortunately, the best solution is irrelative to the weighting factor λ (λ>0) as shown in (16). There is no need to design and choice the weighting factor. The best modulation function is always expressed in (16) in the different weighting factor values. In the actual single-phase converter system, these β-axis components are fictitious quantities to estimate the instantaneous powers. Therefore, only the optimized control variable $u_{ab\alpha}(k)$ is required to achieve the model predictive control, as the input of PWM stage, which can be expressed as

$$u_{ab\alpha}(k) = m(k)u_{\rm dc}(k) \tag{17}$$

where m represents the modulation function. Substituting $u_{ab\alpha}(k)$ of (17) in the first equation of (16), the optimized modulation function can be obtained as (18), as shown bottom of this page.

C. Model Predictive DPC System Structure

Fig. 2 shows the block diagram of the model predictive DPC scheme. In this figure, a PI-based voltage controller is adopted to regulate the dc-link voltage. The output of the PI-based voltage controller multiplied by the dc-link voltage can result the active reference power $P_{\rm ref}$. Reactive reference power $Q_{\rm ref}$ is set to zero for achieving unit power factor. On the basis of SOGI technology, the actual instantaneous active power P and reactive power Q can be obtained from (8), respectively. The MP-DPC scheme is adopted to optimize the modulation function m, as shown in (18). And then, a PWM stage is used to generate the gate signals of power switches, which can keep the switching frequency constant.

As is well known, the model predictive control is particularly sensitive to any model mismatch and to the possibly incorrect identification of the model parameters [42], [43], [49]. MP-DPC of the adopted rectifier is sensitive to its inductance parameter. Thus, the inductance parameter estimation should be discussed. In this paper, the inductance parameter estimation method is shown in (26), which will be discussed in detail, in the next section.

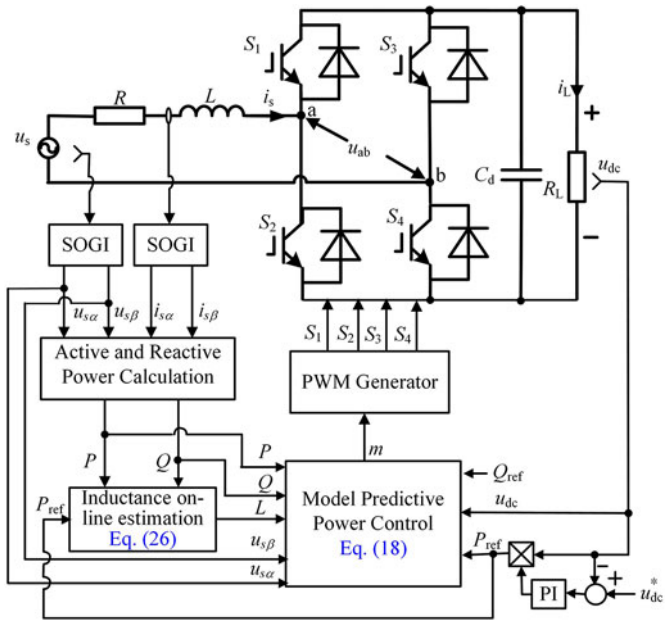

Fig. 2. Block diagram of the proposed model predictive DPC scheme.

D. Inductance Parameter Sensitivity Analysis and Compensation

From (18), the parameter mismatch between the modeled inductance L_m and its actual value L can lead to an estimation error of the modulation function. The estimation error of m will affect the performance of the predictive control system. The impact relationship between the inductance parameter mismatch and the instantaneous power regulation is discussed in the following.

In the MP-DPC controller, the most common option is to use the rated inductance value L_m. Then, on the basis of (11), the differential expressions of active power P and reactive power Q with respect to time t can be shown as

$$\begin{cases} s_p' = \dfrac{{\rm d}P}{{\rm d}t} = \dfrac{1}{2L_m}\left[U_{sm}^2 - u_{s\alpha}u_{ab\alpha} - u_{s\beta}u_{ab\beta}\right] - \omega Q \\ s_q' = \dfrac{{\rm d}Q}{{\rm d}t} = -\dfrac{1}{2L_m}\left[u_{s\beta}u_{ab\alpha} - u_{s\alpha}u_{ab\beta}\right] + \omega P. \end{cases} \tag{19}$$

For the actual converter system, in steady-state condition, the differentiations of active power P and reactive power Q should be zero, and are shown as

$$\begin{cases} s_p = 0 \\ s_q = 0 \end{cases} \Rightarrow \begin{cases} U_{sm}^2 - u_{s\alpha}u_{ab\alpha} - u_{s\beta}u_{ab\beta} = 2L\omega Q \\ u_{s\beta}u_{ab\alpha} - u_{s\alpha}u_{ab\beta} = 2L\omega P. \end{cases} \tag{20}$$

$$m(k) = \frac{u_{s\alpha}(k)U_{sm}^2 T_s + 2\omega L T_s\left[P(k)u_{s\beta}(k) - Q(k)u_{s\alpha}(k)\right] - 2L\left[P_{\rm ref}(k) - P(k)\right]u_{s\alpha}(k) - 2L\left[Q_{\rm ref}(k) - Q(k)\right]u_{s\beta}(k)}{u_{\rm dc}(k)U_{sm}^2 T_s}. \tag{18}$$

TABLE I
ELECTRICAL PARAMETERS OF THE EXPERIMENTAL PROTOTYPE

Parameters	Value
The main voltage(*rms*)	$u_{rms} = 100$ V/50 Hz
DC-link reference voltage	$u_{\rm dc} = 200$ V
Switching frequency	$f_s = 5.0$ kHz
Sampling frequency	$f_c = 10.0$ kHz
the damping factor of SOGI	$k = 1.57$
The rating power	$P_{\rm rating} = 1$ kW
AC-side inductance	$L = 4.7$ mH
DC-link Capacitance	$C_d = 4.4$ mF

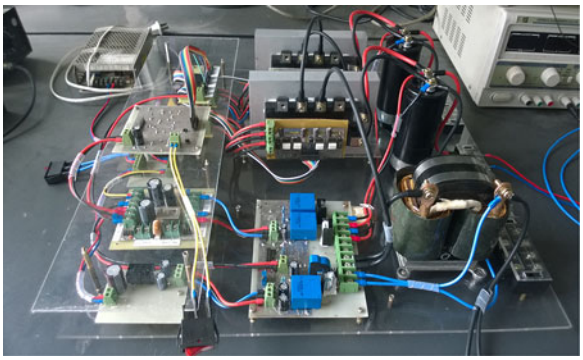

Fig. 3. Photo of the experimental hardware prototype.

Substituting the right side of (20) in (19), the differential expressions of P and Q in the MP-DPC controller are deduced and discretized as

$$\begin{cases} s_p' = \dfrac{P(k+1)-P(k)}{T_s} = \left(\dfrac{L}{L_m}-1\right)\omega Q(k) \\ s_q' = \dfrac{Q(k+1)-Q(k)}{T_s} = \left(1-\dfrac{L}{L_m}\right)\omega P(k). \end{cases} \tag{21}$$

Depending on (8), the actual active power $P(k)$ and reactive power $Q(k)$ estimated at the kth interval, are insensitive to the inductance mismatch. But inductance mismatch will result the prediction error of active power $P(k+1)$ and reactive power $Q(k+1)$ estimation as shown in (21). As is shown in Fig. 2, a dc-link voltage PI controller is adopted to generate the desirable reference active power $P_{\rm ref}(k)$. So even if there is a prediction error of active power in the power control inner loop, the dc-link voltage control loop can correct the error, and force the actual active power to track the desirable reference active power. It means that there is no effect on the active power P even if the inductance parameter mismatches.

It is assumed that the actual reactive power $Q(k+1)$ at the $(k+1)$th interval reaches the reference value $Q_{\rm ref}(k)$ at the kth control interval. The second expression of (21) can be rewritten as

$$Q(k+1) = Q_{\rm ref}(k) = Q(k) + \omega P(k) T_s \left(1 - \frac{L}{L_m}\right). \tag{22}$$

Unfortunately, the reference reactive power $Q_{\rm ref}(k)$ is set as zero to achieve unit power factor. Therefore, the reactive power

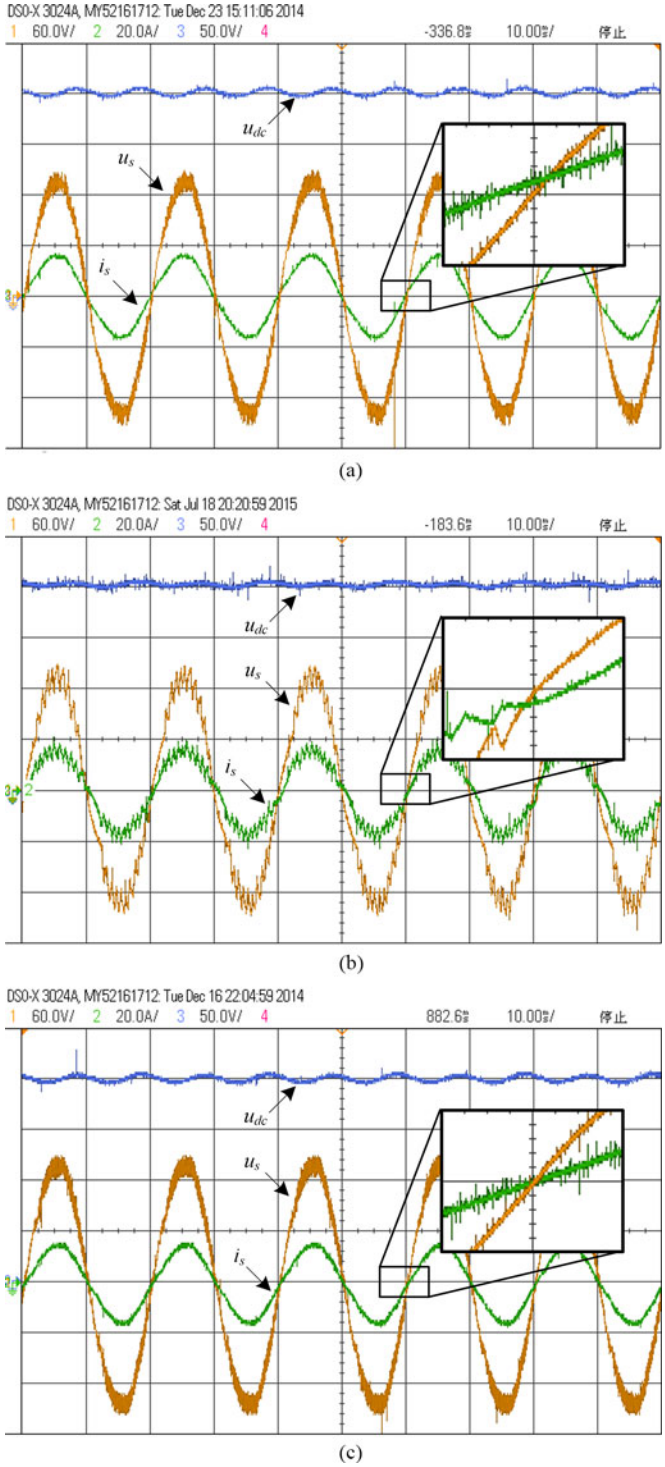

Fig. 4. Experimental waveforms of the main voltage, the line current and dc-link capacitor voltage in steady state. ($u_{\rm dc}$: 50V/div, u_s: 60V/div, i_s: 20A/div, Time: 10 ms/div). (a) Conventional PI-based ICC. (b) FCS-MP-DPC. (c) Proposed MP-DPC.

caused by the inductance mismatch, and can be expressed as

$$Q(k) = \omega P(k) T_s \left(\frac{L}{L_m} - 1\right). \tag{23}$$

The aforementioned analysis results demonstrate that ac-side inductance mismatch can lead to reactive power offset, whose

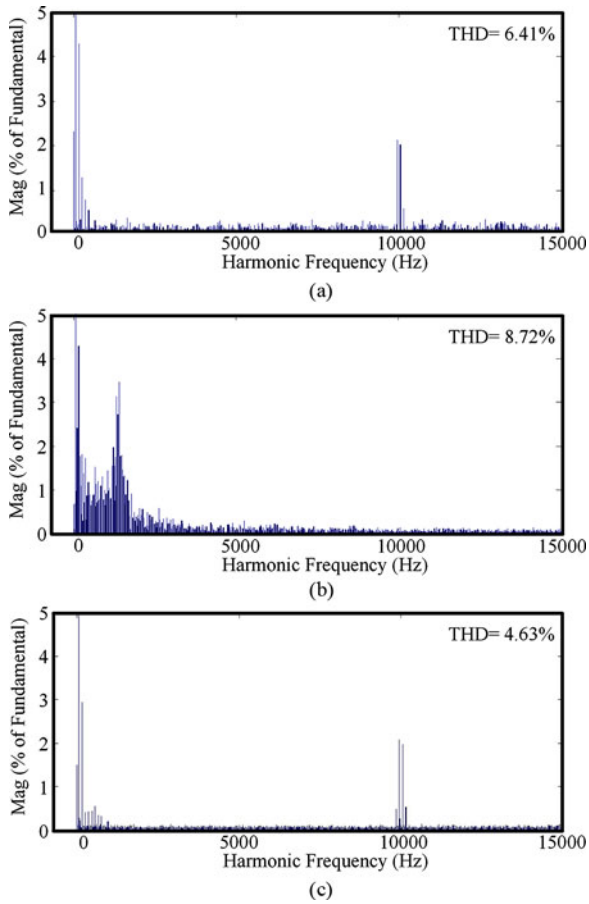

Fig. 5. FFT analysis of the line currents in experiment test. (a) Conventional PI-based ICC. (b) FCS-MP-DPC. (c) Proposed MP-DPC.

value depends on the switching period T_s and the active power P. Depending on (23), if the estimating inductance L_m is larger than the actual inductance L, the estimation error will result that a negative reactive power occurs in the adopted converter. Otherwise, if L_m is smaller than the actual value L, a positive reactive power occurs in the adopted converter. In order to eliminate the reactive power offset caused by inductance mismatch, the best solution is to estimate the online inductance, which is shown as follows.

First, the inductance mismatch ratio δ is defined as

$$\delta = \frac{L_m}{L} - 1. \tag{24}$$

Substituting (24) into (23), (23) can be rewritten as

$$Q(k) = -\frac{\delta}{1+\delta}\omega P(k) T_s. \tag{25}$$

On the basis of (23), the inductance online estimation can be shown as

$$L(k) = \begin{cases} \left[\dfrac{Q(k)}{\omega P(k) T_s} + 1\right] L(k-1) & k = 1, 2, 3.... \\ L_m & k = 0. \end{cases} \tag{26}$$

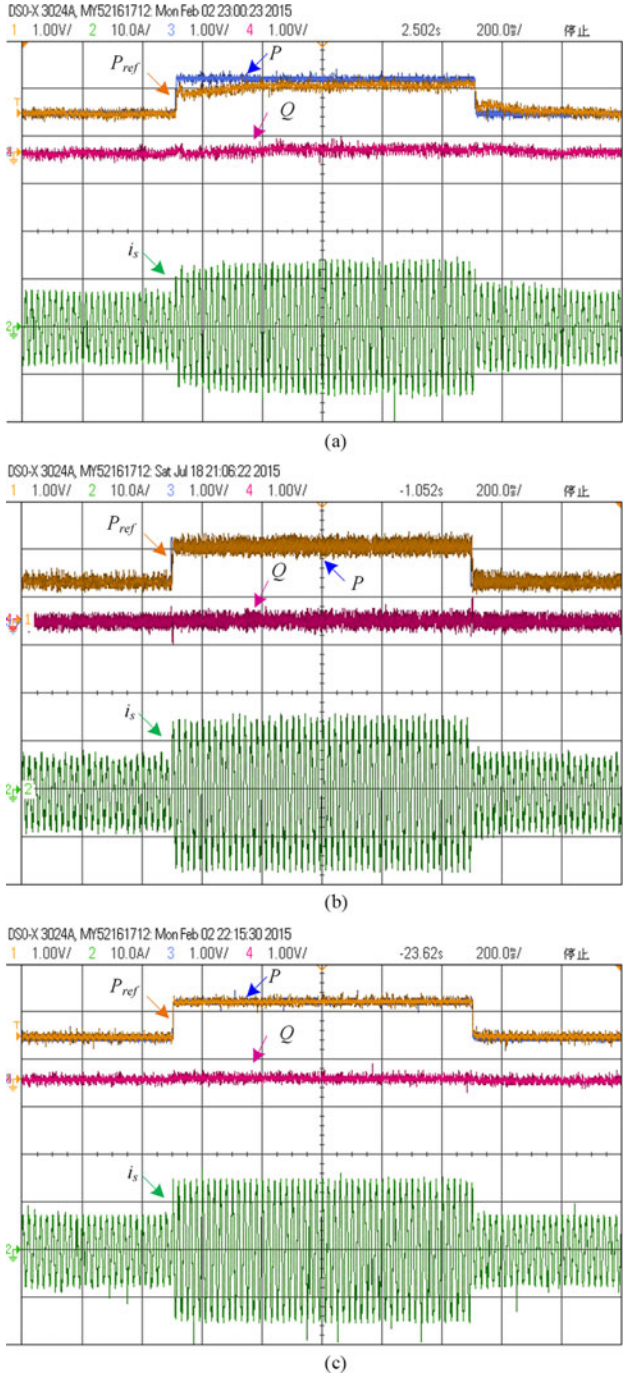

Fig. 6. Experimental waveforms of dynamic response of active and reactive powers regulation when active power reference step up from 50% to 100% rating value and vice verse after 1.0 s (P and $P*$: 640W/div, Q: 640 var/div, i_s: 10A/div, Time: 200 ms/div). (a) Conventional PI-Based ICC. (b) FCS-MP-DPC. (c) Proposed MP-DPC.

Due to the active and reactive ripple, a low-pass filter should be adopted to keep the estimated inductance value smooth in the practical application.

V Experimental Results

In order to verify the effectiveness of the proposed system, a single-phase two-level rectifier experimental prototype has

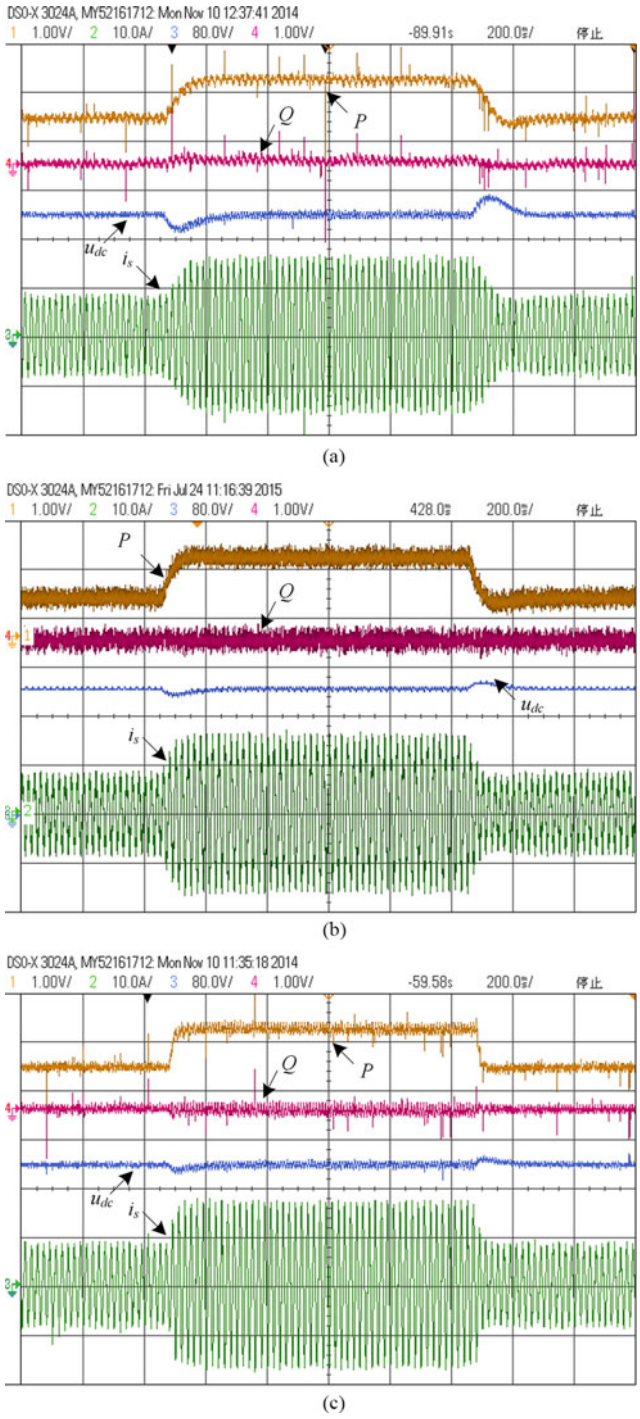

Fig. 7. Experimental waveforms of dynamic response of active and reactive powers regulation when a load steps from 50% to full load and vice versa after 1.0s (*P*: 640W/div, *Q*: 640 var/div, $u_{\rm dc}$: 80V/div, i_s: 10A/div, Time: 200 ms/div). (a) Conventional PI-based ICC. (b) FCS-MP-DPC. (c) Proposed MP-DPC.

TABLE II
DYNAMIC RESPONSE OF DC-LINK VOLTAGE IN LOAD STEP-UP CONDITION

Performance \ Control Schemes	PI-Based ICC	FCS MP-DPC	The Proposed MP-DPC
Voltage dip	16%	10.5%	8%
Overshoot peak response	50 ms	35 ms	30 ms
Settling time	180 ms	160 ms	150 ms

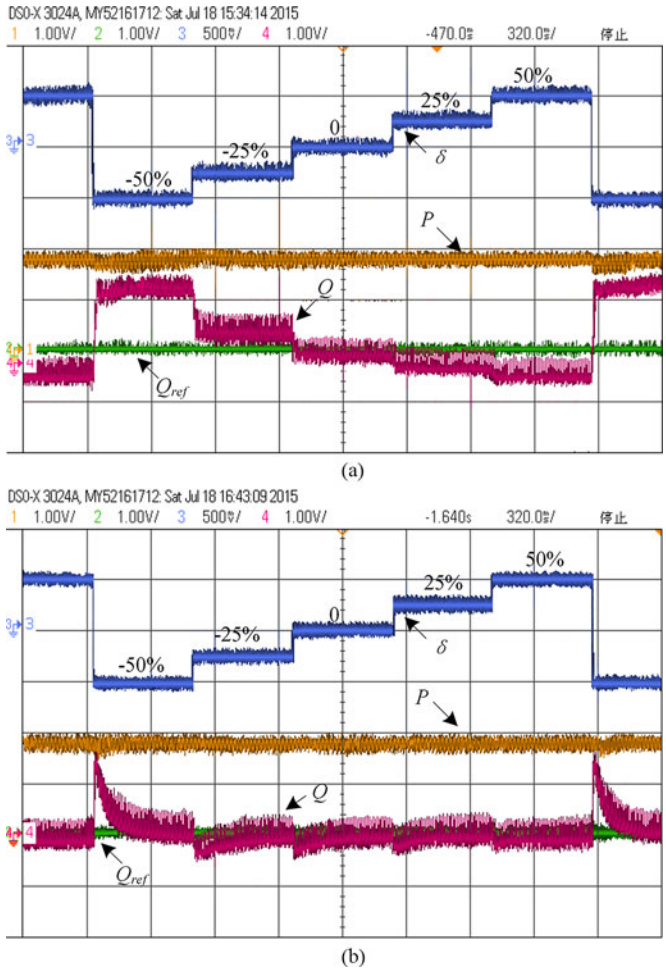

Fig. 8. Experimental waveforms of the inductance mismatch ratio δ, the active and reactive powers while δ steps from –50% to +50% with and without compensation schemes (*P*: 640 W/div, *Q*: 160 var/div, i_s: 10 A/div, Time: 320 ms/div). (a) Noncompensation for inductance mismatch. (b) Compensation for inductance mismatch.

been implemented. The steady-state and dynamic performances of the proposed MP-DPC are compared to those of the PI-based ICC and the conventional FCS-MP-DPC[42], [43] schemes. The electrical parameters of the experimental prototype are shown in Table I. The damping factor *k* has an effect on the settling time of SOGI. In order to obtain the minimum settling time of SOGI for extracting the 50-Hz sinusoidal signals, the damping factor *k* should be set to 1.57. The detail certification is reported in [48].

A. *Experimental Platform*

The photo of the experimental hardware prototype platform is shown in Fig. 3. It consists of the main IPM power circuit, the sensor sampling and signal processing circuit, Texas Instruments TMS320F2812 controller, gate signal driving and protecting circuit, and so on. The H-bridge IPM module in the main power circuit is Mitsubishi PM50B4LA060 with the maximum switching frequency 20 kHz. Two LEM LV 25-P Hall voltage sensors and one LEM LTS 25-NP Hall current sensor are used in sensor sampling circuit. A logical interlock and dead-time

TABLE III
REACTIVE POWER VALUES IN INDUCTANCE MISMATCH CONDITION

Inductance mismatch ratio $\delta = L_m / L - 1$	-50%	-25%	0	25%	50%
The average reactive power ratio (Q/P) estimated from (23)	6.3%	2.1%	0	-1.3%	-2.1%
The average reactive power ratio (Q/P) measured from simulations	6.3%	1.9%	0.3%	-1.5%	-2.4%
The average reactive power error ratio(Q/P) measured in experiments	5.0%	3.2%	0	-1.6%	-2.7%

function are designed in PWM signal processing and protecting circuit.

B. Steady-State Performance Comparison

Fig. 4(a)–(c) show experimental waveforms of the main voltage, the line current, and dc-link voltage for the PI-based ICC, FSC-MP-DPC, and the proposed MP-DPC schemes in steady state, respectively. There are some harmonic pulse voltages in the waveforms of the main voltages, due to the inductance of an autotransformer as power supply in the experimental prototype. From the experiments, it is observed that the line currents are drawn to be sinusoidal in phase with the main voltages in these three control schemes, approximately. But waveform quality of the line current in FCS-MP-DPC scheme is worst, due to limitation of the sampling and control frequency ($f_c = 10$ kHz). Compared with the partial enlarged details shown in Fig. 4(a)–(c), the proposed MP-DPC scheme can obtain zero power factor angle and unit displacement power factor (DPF). But DPF values are lower than 1 in both of PI-based ICC and the traditional MP-DPC, as shown in Fig. 4(a) and (b). The reason is that there is always a steady-state current error in PI-based ICC scheme, and the control frequency $f_c = 10$ kHz is a bit low and difficult to achieve unit DPF for FSC-MP-DPC implemented in DSP TMS320F2812 chip.

Fig. 5 shows experimental FFT results of the line currents. It can be noticed that, due to only one switching state adopted during the whole control period in FCS-MP-DPC, the current total harmonic distortion (THD) is 8.87% and higher than two other schemes in the same control frequency condition. In Fig. 5(b), the current harmonics distribute widely in the frequency domain, due to the inherent drawback of FCS-MP-DPC: variable switching frequency. Compared with Fig. 5(a) and (c), high-order harmonics of the line currents in PI-based ICC and the proposed MP-DPC schemes, distribute around the twice switching frequencies $2f_s$, due to the PWM module with the same switching frequency adopted in both of control systems. It is clear that the proposed MP-DPC can achieve much lower current THD and less current harmonics than PI-based ICC. Therefore, the proposed MP-DPC can obtain the lowest current THD, and remain constant switching frequency in these three control schemes.

C. Dynamic Response Performance Comparison

To test dynamic response of active and reactive powers regulation under power step change condition, Fig. 6 shows experimental waveforms of active power P and $P_{\rm ref}$, reactive power Q, and the line current i_s, when active power command $P_{\rm ref}$ steps up from 50% to 100% rating value and vice versa at the instant after 1.0 s. From Fig. 6, a comparison of active power P and reactive power Q shows that dynamic response of power regulation in two MP-DPC methods are better than those in the conventional PI-based ICC. And MPC-DPC methods can eliminate the instantaneous powers' stead-state errors more effectively than the PI-based ICC. However, power ripples in FCS-MP-DPC are much larger than those in the proposed MP-DPC. Thus, the proposed MP-DPC cannot only retain the fast-transient response of the traditional MP-DPC, but also obtain the high precise power value with smaller ripple.

Fig. 7 shows experimental waveforms of dynamic response of dc-link voltage when a load is scheduled to step from 50% to full load and vice versa at the instant after 1.0 s. Table II shows a dynamic response comparison of dc-link voltage in load step-up condition. The dynamic response of dc-link voltage depends on the PI voltage controller and inner power or current controller. In this paper, the same voltage PI parameters are adopted in these three methods. Thus, in the theory, the dynamic response of these two MP-DPC schemes should be faster than PI-based ICC, due to the faster dynamic response of an inner power controller verified in Fig. 6. Therefore, it is clear that, in the same sampling and control frequency condition, the proposed MP-DPC scheme can obtain a faster dynamic response than PI-based ICC, and retain the advantage of fast dynamic response in FCS-MP-DPC scheme, from a comparison of experimental results shown in Fig. 7 and Table II.

D. Experimental Sensitivity Analysis

Fig. 8(a) shows experimental waveforms of the active and reactive powers in the proposed MP-DPC while the inductance mismatch ratio δ steps up from -50%, -25%, 0, 25% to 50%. It can be noticed that, the larger the absolute value of the inductance mismatch ratio δ is, the higher the reactive power is. And the negative ratio δ can result more reactive power than the positive ratio δ in case of the same absolute value of ratio δ, which is coincided with (25).

And Fig. 8(b) shows the corresponding experimental waveforms with online estimation scheme of inductance parameter. A comparison of Fig. 8(a) and (b) can verify the inductance estimation scheme can eliminate the inductance mismatch influence on the reactive power Q, effectively. In additional, there is no effect on the active power P.

Table III shows the comparison of the reactive power values in theoretical calculation from (23), simulation and experimental tests with different inductance mismatch ratios. Comparison results verify the correctness of theoretical analysis.

TABLE IV
PERFORMANCE COMPARISON OF THREE CONTROL SCHEMES

Performances \ Control Schemes	PI-Based ICC	FCS-MP-DPC	The Proposed MP-DPC
Power factor angle	7.2°	4°	0°
THD	6.41%	8.72%	4.63%
Inner-loop settling time	300 ms	<10 ms	<10 ms
Inner-loop static error	Yes	No	No
Switching frequency	constant	variable	constant
PI controller number	2	1	1
Weight factor of cost function	—	relative	irrelative

VI. CONCLUSION

A model predictive direct power control (MP-DPC) with the modulation function optimization for the instantaneous power regulation of single-phase PWM rectifiers is proposed in this paper. On the basis of SOGI, the instantaneous active and reactive powers solution of single-phase converters is discussed in two-phase stationary coordinate frame. The optimized modulation function of the adopted rectifier is obtained from the cost function minimization in MP-DPC. The proposed MP-DPC scheme combined with the PWM stage constitutes the overall control system of the adopted rectifier. And the sensitivity of the MP-DPC scheme is investigated, due to the ac-side inductor parameter mismatch. On the basis of this, the inductance parameter online estimation scheme is proposed to eliminate its effect on the reactive power. The performance of the proposed MP-DPC scheme is evaluated based on a single-phase PWM rectifier scale-down experiment test. Moreover, it was compared with that of the conventional PI-based instantaneous current control (ICC) approach widely adopted in the railway traction application, and the finite-control-set (FCS) MP-DPC scheme. And Table IV shows a performance comparison of these three control schemes on the basis of experimental results and theoretical analysis.

The conducted studies conclude that the proposed method is characterized by the following.

1) Compared with FCS-MP-DPC, the proposed MP-DPC scheme using PWM can reduce current harmonic components and THD, obtain a constant switching frequency, and remain the advantage of fast dynamic response in FCS-MP-DPC.
2) Compared with the conventional PI-based ICC scheme, the MP-DPC scheme is free of complicated multiple PI controllers design, can achieve zero steady-state power errors, faster dynamic response for powers and dc-link voltage.
3) Compared with FCS-MP-DPC, the proposed MP-DPC scheme is irrelative to the weighting factor of cost function.
4) The disadvantage of the proposed MP-DPC scheme is that the reactive power is relative to ac-side inductor parameter mismatch. The quantitative expression of reactive power caused by inductance mismatch is achieved and verified by simulation and experimental results.
5) On the basis of the quantitative expression of reactive power with inductance parameter, the proposed the inductance parameter online estimation scheme can effectively eliminate the effect on reactive power, caused by inductance mismatch.

REFERENCES

[1] P. T. Krein, R. S. Balog, and M. Mirjafari, "Minimum energy and capacitance requirements for single-phase inverters and rectifiers using a ripple port," *IEEE Trans. Power Electron.*, vol. 27, no. 11, pp. 4690–4698, Nov. 2012.

[2] B.-R. Lin and T.-Y. Yang, "Single-phase switching mode multilevel rectifier with a high power factor," *Proc. IEE*, May 2005, vol. 152, no. 3, pp. 447–454.

[3] H. Komurcugil, N. Altin, S. Ozdemir, and I. Sefa, "An extended Lyapunov-function-based control strategy for single-phase UPS inverters," *IEEE Trans. Power Electron.*, vol. 30, no. 7, pp. 3976–3983, Jul. 2015.

[4] A. B. Youssef, S. K. E. Khil, and I. Slama-Belkhodja, "State observer-based sensor fault detection and isolation, and fault tolerant control of a single-phase PWM rectifier for electric railway traction," *IEEE Trans. Power Electron.*, vol. 28, no. 12, pp. 5842–5853, Dec. 2013.

[5] W. Song, S. Wang, C. Xiong, X. Ge, and X. Feng, " Single phase three-level SVPWM algorithm for grid-side railway traction converter and its relationship of carrier-based PWM," *IET Electr. Syst. Transp.*, vol. 4, no. 3, pp. 78–87, 2014.

[6] V. B. Sriram, S. SenGupta, and A. Patra, "Indirect current control of a single-phase voltage-sourced boost-type bridge converter operated in the rectifier mode," *IEEE Trans. Power Electron.*, vol. 18, no. 5, pp. 1130–1137, May 2003.

[7] P. A. Dahono, "New hysteresis current controller for single-phase full bridge inverters," *IET Power Electron.*, vol. 2, no. 5, pp. 585–594, 2009.

[8] M. Brenna, F. Foiadelli, and D. Zaninelli, "New stability analysis for tuning PI controller of power converters in railway application," *IEEE Trans. Ind. Electron.*, vol. 58, no. 2, pp. 533–543, Feb. 2011.

[9] H-. S. Song, R. Keil, P. Mutschler, J. Van Der Weem, and K. Nam, "Advanced control scheme for a single-phase PWM rectifier in traction applications," in *Proc. IEEE IAS Annu. Meet.*, 2003, vol. 3, pp. 1558–1565.

[10] D. N. Zmood and D. G. Holmes, "Stationary frame current regulation of PWM inverters with zero steady-state error," *IEEE Trans. Power Electron.*, vol. 18, no. 3, pp. 814–822, May 2003.

[11] B. Bahrani, A. Rufer, S. Kenzelmann, and L. A. C. Lopes, "Vector control of single-phase voltage-source converters based on fictive-axis emulation," *IEEE Trans. Ind. Appl.*, vol. 47, no. 2, pp. 831–840, Mar. /Apr. 2011.

[12] Y. Nishida, O. Miyashita, T. Haneyoshi, H. Tomita, and A. Maeda, "A predictive instantaneous-current PWM controlled rectifier with AC-side harmonic current reduction," *IEEE Trans. Ind. Electron.*, vol. 44, no. 3, pp. 337–343, Jun. 1997.

[13] W. Song, X. Feng, and K. M. Smedley, "A carrier-based PWM strategy with the offset voltage injection for single-phase three-level neutral-point-clamped converters," *IEEE Trans. Power Electron.*, vol. 28, no. 3, pp. 1083–1095, Mar. 2013.

[14] M. Azab, "A new direct power control of single phase PWM boost converter," in *Proc. IEEE 46th Midwest Symp. Circuits Syst. Conf.*, 2003, pp. 1081–1084.

[15] K. G. Pavlou, M. Vasiladiotis, and S. N. Manias, "Constrained model predictive control strategy for single-phase switch-mode rectifiers," *IET Power Electron.*, vol. 5, no. 1, pp. 31–40, Jan. 2012.

[16] M. Monfared, M. Sanatkar, and S. Golestan, "Direct active and reactive power control of single-phase grid-tie converters," *IET Power Electron.*, vol. 5, no. 8, pp. 1544–1550, Aug. 2012.

[17] H. Akagi, Y. Kanazawa, and A. Nabae, "Instantaneous reactive power compensators comprising switching devices without energy storage components," *IEEE Trans. Ind. Appl.*, vol. IA-20, no. 3, pp. 625–630, Sep. 1984.

[18] T. Noguchi, H. Tomiki, S. Kondo, and I. Takahashi, "Direct power control of PWM converter without power-source voltage sensors," *IEEE Trans. Ind. Appl.*, vol. 34, no. 3, pp. 473–479, May/Jun. 1998.

[19] B. S. Chen and G. Joos, "Direct power control of active filters with averaged switching frequency regulation," *IEEE Trans. Power Electron.*, vol. 23, no. 6, pp. 2729–2737, Jun. 2008.

[20] J. G. Norniella, J. M. Cano, G. A. Orcajo, C. H. Rojas, J. F. Pedrayes, M. F. Cabanas, and M. G. Melero, "Improving the dynamics of virtual flux

based control of three-phase active rectifiers," *IEEE Trans. Ind. Electron.*, vol. 61, no. 1, pp. 177–187, Jan. 2014.
[21] A. Bouafia, F. Krim, and J.-P. Gaubert, "Fuzzy-logic-based switching sate selection for direct power control of three-phase PWM rectifier," *IEEE Trans. Ind. Electron.*, vol. 56, no. 6, pp. 1984–1992, Jun. 2009.
[22] A. Bueno, J. M. Aller, J. A. Restrepo, R. Harley, and T. G. Habetler, "Harmonic and unbalance compensation based on direct power control for electric railway systems," *IEEE Trans. Power Electron.*, vol. 28, no. 12, pp. 5823–5831, Dec. 2013.
[23] J. Hu and Z. Q. Zhu, "Investigation on switching patterns of direct power control strategies for grid-connected DC-AC converters based on power variation rates," *IEEE Trans. Power Electron.*, vol. 26, no. 12, pp. 3582–3598, Dec. 2011.
[24] P. R. Martinez-Rodriguez, G. Escobar, A. A. Valdez-Fernandez, M. Hernandez-Gomez, and J. M. Sosa, "Direct power control of a three-phase rectifier based on positive sequence detection," *IEEE Trans. Ind. Electron.*, vol. 61, no. 8, pp. 4084–4092, Aug. 2014.
[25] Y. Zhang, Z. Li, Y. Zhang, W. Xie, Z Piao, and C Hu, "Performance improvement of direct power control of PWM rectifier with simple calculation," *IEEE Trans. Power Electron.*, vol. 28, no. 7, pp. 3428–3437, Jul. 2013.
[26] M. Malinowski, M. Jasinski, and M. P. Kazmierkowski, "Simple direct power control of three-phase PWM rectifier using space-vector modulation (DPC-SVM)," *IEEE Trans. Ind. Electron.*, vol. 51, no. 2, pp. 447–454, Apr. 2004.
[27] C. E. Capovilla, I. R. S. Casella, A. J. S. Filho, T. A. Dos, S. Barros, and E. R. Filho, "Performance of a direct power control system using coded wireless OFDM power reference transmissions for switched reluctance aerogenerators in a smart grid scenario," *IEEE Trans. Ind. Electron.*, vol. 62, no. 1, pp. 52–61, Jan. 2015.
[28] J. Hu, L. Shang, Y. He, and Z. Q. Zhu, "Direct active and reactive power regulation of grid-connected DC/AC converters using sliding mode control approach," *IEEE Trans. Ind. Electron.*, vol. 26, no. 1, pp. 210–222, Jan. 2011.
[29] A. Bouafia, J. P. Gaubert, and F. Krim, "Predictive direct power control of three-phase pulse width modulation (PWM) rectifier using space-vector modulation (SVM)," *IEEE Trans. Power Electron.*, vol. 25, no. 1, pp. 228–236, May. 2010.
[30] J. R. Fischer, S. A. Gonzlez, I. Carugati, M. A. Herran, M. G. Judewicz, and D. O. Carrica, "Robust predictive control of grid-tied converters based on direct power control," *IEEE Trans. Power Electron.*, vol. 29, no. 10, pp. 5634–5643, Oct. 2014.
[31] W. Song, J. Ma, L. Zhou, and X. Feng, "Deadbeat predictive power control of single-phase three-level neutral-point-clamped converters using space-vector modulation for electric railway traction," *IEEE Trans. Power Electron.*, vol. 31, no. 1, pp. 721–732, Jan. 2016.
[32] D. Choi and K. Lee, "Dynamic performance improvement of AC/DC converter using model predictive direct power control with finite control set," *IEEE Trans. Ind. Electron.*, vol. 62, no. 2, pp. 757–767, Feb. 2015.
[33] S. Kwak, U.-C. Moon, and J.-C. Park, "Predictive control based direct power control with an adaptive parameter identification technique for improved AFE performance," *IEEE Trans. Power Electron.*, vol. 29, no. 10, pp. 6178–6187, Nov. 2014.
[34] Y. Zhang, J. Hu, and J. Zhu, "Three-vectors-based predictive direct power control of the doubly fed induction generator for wind energy applications," *IEEE Trans. Power Electron.*, vol. 29, no. 7, pp. 3485–3500, Dec. 2014.
[35] Z. Song, W. Chen, and C. Xia, "Predictive direct power control for three-phase grid-connected converters without sector information and voltage vector selection," *IEEE Trans. Power Electron.*, vol. 29, no. 10, pp. 5518–5531, Oct. 2014.
[36] R. Portillo, S. Vazquez, J. I. Leon, M. M. Prats, and L. G. Franquelo, "Model based adaptive direct power control for three-level NPC converters," *IEEE Trans. Ind. Informat.*, vol. 9, no. 2, pp. 1148–1156, May 2013.
[37] S. Vazquez, J. A. Sanchez, J. M. Carrasco, J. I. Leon, and E. Galvan, "A model-based direct power control for three-phase power converters," *IEEE Trans. Ind. Electron.*, vol. 55, no. 4, pp. 1647–1657, Apr. 2008.
[38] Y. Zhang, W. Xie, Z. Li, and Y. Zhang, "Model predictive direct power control of a PWM rectifier with duty cycle optimization," *IEEE Trans. Power Electron.*, vol. 28, no. 11, pp. 5343–5351, Nov. 2013.
[39] P. Cortes, J. Rodriguez, P. Antoniewicz, and M. Kazmierkowski, "Direct power control of an AFE using predictive control," *IEEE Trans. Power Electron.*, vol. 23, no. 5, pp. 2516–2523, Sep. 2008.
[40] J. A. Restrepo, J. M. Aller, J. C. Viola, A. Bueno, and T. G. Habetler, "Optimum space vector computation technique for direct power control," *IEEE Trans. Power Electron.*, vol. 24, no. 6, pp. 1637–1645, Jun. 2009.
[41] S. Vazquez, A. Marquez, R. Aguilera, D. Quevedo, J. I. Leon, and L. G. Franquelo, "Predictive optimal switching sequence direct power control for grid connected power converters," *IEEE Trans. Ind. Electron.*, vol. 62, no. 4, pp. 2010–2020, Apr. 2015.
[42] J. Redriguez and P. Cortes, *Predictive Control of Power Converters and Electrical Drives*. Hoboken, NJ, USA: Wiley, 2012.
[43] S. Kouro, P. Cortés, R.Vargas, U. Ammann, and J. Rodríguez, "Model predictive control—A simple and powerful method to control power converters," *IEEE Trans. Ind. Electron.*, vol. 56, no. 6, pp. 1826–1838, Jun. 2009.
[44] S. Vazquez, J. I. Leon, L. G. Franquelo, J. M. Carrasco, O. Martinez, J. Rodriguez, P. Cortes, and S. Kouro, "Model Predictive Control with constant switching frequency using a Discrete Space Vector Modulation with virtual state vectors," in *Proc. IEEE Int. Conf. Ind. Technol.*, Feb. 2009, pp. 1–6.
[45] M. Gonzalez, V. Cardenas, and F. Pazos, "DQ transformation development for single-phase systems to compensate harmonic distortion and reactive power," in *Proc. IEEE Int. Power Electron. Congr.*, Oct. 2004, pp. 177–182.
[46] S. Nakoto, M. Mobuyuki, and S. Toshihisa, "A control strategy of single phase active filter using a novel d-q transformation," presented at the IEEE 38th Industry Applications Society Annu. Meet., Salt Lake City, UT, USA, 2003.
[47] B. H. Kwon, J. H. Choi, and T. W. Kim, "Improved single-phase line interactive UPS," *IEEE Trans. Ind. Electron.*, vol. 48, no. 4, pp. 804–811, Aug. 2001.
[48] A. Kulkarni and V. John, "A novel design method for SOGI-PLL for minimum settling time and low unit vector distortion," in *Proc. IEEE Ind. Electron. Soc. Conf.*, Nov. 2013, pp. 274–279.
[49] J. G. Norniella, J. M. Cano, G. A. Orcajo, C. Garcia, J. F. Pedrayes, M. F. Cabanas, and M. G. Melero, "Analytic and iterative algorithms for online estimation of coupling inductance in direct power control of three-phase active rectifiers," *IEEE Trans. Power. Electron.*, vol. 26, no. 11, pp. 3298–3307, Nov. 2011.

Wensheng Song (M'13) received the B.S. degree in electronic and information engineering and the Ph.D. degree in electrical engineering from Southwest Jiaotong University, Chengdu, China, in 2006 and 2011, respectively.

He is currently a Lecturer in the school of Electrical Engineering, Southwest Jiaotong University. From September 2009 to September 2010, he was a Visiting Scholar with the Department of Electrical Engineering and Computer Science, University of California, Irvine, CA, USA. From July 2015 to December 2015, he is a Visiting Scholar at the University of Alberta, Edmonton, Canada. His current research interests include digital control and modulation methods of electrical ac–dc–ac railway traction drive systems, and multilevel converters.

Zhixian Deng was born in Jiujiang, Jiangxi, China, in 1990. He received the B.S. degree in electrical engineering from Southwest Jiaotong University, Chengdu, china, in 2013, where he is currently working toward the M.S degree in electrical engineering.

His current research interests include digital control and modulation of power converters in railway application.

ShunLiang Wang was born in Sichuan, China, in 1987. He received the B.S. degrees in electrical engineering from Southwest Jiaotong University, Chengdu, China, in 2010, where he is currently working toward the Ph.D. degree in electrical engineering.

His current research interests include digital control and modulation of power converters, multilevel converters, and power electronic transformers in railway application.

Xiaoyun Feng received the B.S., M.S., and Ph.D. degrees in electrical engineering from Southwest Jiaotong University, Chengdu, China, in 1983, 1988, and 2001, respectively.

Since 1983, she has been with the College of Electrical Engineering, Southwest Jiaotong University, where she is currently a Full Professor. She was a Visiting Professor at the University of Tokyo, between October 1998 and October 1999. She is the author or coauthor of more than 70 papers. Her main research interest includes the analysis and control of electrical traction converter and motor drive system, the design of railway traction characteristics, and railway train optimizing operation.